Silicate Emission in the *Spitzer*[1] IRS[2] spectrum of FSC 10214+4724

H. I. Teplitz[3], L. Armus[3], B.T. Soifer[3], V. Charmandaris[4,5,6], J. A. Marshall[4], H. Spoon[4], C. Lawrence[7], L. Hao[4], S. Higdon[4], Y. Wu[4], M. Lacy[3], P. R. Eisenhardt[7], T. Herter[4], J.R. Houck[4]

ABSTRACT

We present the first MIR spectrum of the $z = 2.2856$ ultraluminous, infrared galaxy FSC 10214+4724, obtained with the Infrared Spectrograph onboard the *Spitzer Space Telescope*. The spectrum spans a rest wavelength range of $2.3 - 11.5\mu$m, covering a number of key diagnostic emission and absorption features. The most prominent feature in the IRS spectrum is the silicate emission at restframe ~ 10 μm. We also detect an unresolved emission line at a rest wavelength of 7.65μm which we identify with [NeVI], and a slightly resolved feature at 5.6 μm identified as a blend of [Mg VII] and [Mg V]. There are no strong PAH emission features in the FSC 10214+4724 spectrum. We place a limit of 0.1μm on the equivalent width of 6.2μm PAH emission but see no evidence of a corresponding 7.7 μm feature. Semi-empirical fits to the spectral energy distribution suggest $\sim 45\%$ of the bolometric luminosity arises from cold (~ 50 K) dust, half arises from warm (190 K) dust, and the remainder, $\sim 5\%$ originates from hot (~ 640 K) dust. The hot dust is required to fit the blue end of the steep MIR spectrum. The combination of a red continuum, strong silicate emission, little or no PAH emission, and no silicate absorption, makes FSC 10214+4724 unlike most other ULIRGs or AGN observed thus far with IRS. These apparently contradictory

properties may be explained by an AGN which is highly magnified by the lens, masking a (dominant) overlying starburst with unusually weak PAH emission.

Subject headings: cosmology: observations — galaxies: evolution — galaxies: high-redshift — galaxies: individual (FSC 10214+4724)

1. Introduction

FSC 10214+4724, at a redshift of $z = 2.2856$ (Rowan-Robinson et al. 1991), was initially thought to be the most luminous object in the Universe, but was later revealed to be gravitationally lensed by a foreground galaxy (Broadhurst & Lehar 1995; Graham & Liu 1995; Serjeant et al. 1995; Eisenhardt et al. 1996). The lensing model of Eisenhardt et al. (1996) suggests that the central (optical/UV) source is magnified by a factor of ~ 100, and that the lensing arc is an image of the central $\sim 0''.005$ (40 pc) of the source at B-band rest wavelength. They further conclude that the bolometric luminosity of the source is produced over a larger region (240 pc), implying a bolometric magnification factor of 30 and an intrinsic luminosity of $\sim 2 \times 10^{13}$ $L_\odot$, placing it in the class of ultraluminous infrared galaxies (ULIRGs). The large magnification makes FSC 10214+4724 a unique subject for the study of high redshift ULIRGs, offering greater effective sensitivity and spatial resolution than possible in observations of unlensed sources.

A central question in understanding FSC 10214+4724 is the relative contribution of starburst and AGN components to its luminosity. The rest-frame UV-optical spectrum appears to be similar to that of Seyfert 2 galaxies (Elston et al. 1994). Strong UV polarization shows that much of the UV continuum results from scattered light, and broad lines in the polarization spectrum identify the presence of an AGN (Lawrence et al. 1993; Goodrich et al. 1996). The bulk of the luminosity, however, is emitted in the infrared (as much as 99%, Rowan-Robinson et al. 1991). CO observations point to a large reservoir of molecular gas (Solomon et al. 1992; Scoville et al. 1995). Sub-mm and millimeter detections (Downes et al. 1992; Rowan-Robinson et al. 1993; Benford et al. 1999) suggest substantial emission from cold dust, usually associated with extended star formation. Recent *Chandra* observations show the object to have weak X-ray emission, consistent with vigorous star formation or a Compton-thick AGN (Alexander et al. 2005). Lens models suggest differential amplification, so that the central (AGN-dominated) region is more highly magnified than the surrounding starburst (e.g., Eisenhardt et al. 1996; Lacy et al. 1998).

The sensitivity and large wavelength coverage of the *Spitzer* Infrared Spectrograph (IRS Houck et al. 2004) makes it possible to explore the dust emission and absorption features

in the rest-frame mid-infrared spectra of dusty galaxies at low and high redshift, and thus identify the power sources which may be hidden in the UV and optical. In this paper, we present the first MIR spectrum of FSC 10214+4724. We describe the observations and data reduction in Section 2, present the spectrum and a dust emission model fit to the spectral energy distribution in Section 3, and discuss the implications in Section 4. Throughout, we assume a Λ-dominated flat universe, with $H_0 = 70$ km s^{-1} Mpc^{-1}, $\Omega_\Lambda = 0.7, \Omega_m = 0.3$.

2.   Observations and Data Reduction

Spectra of FSC 10214+4724 were obtained with the IRS on 19 April 2004. The data were taken in the first order of the low resolution, short wavelength module (SL-1; 7.5-14.2 μm) and in both orders of the low resolution, long wavelength module (LL-1 and LL-2, 14.2-21.8 and 20.6-38 μm, respectively). The spectral resolution varies from 60 to 120 across each order. Individual ramp durations were 60 seconds in SL-1 and 120 in LL-1 and LL-2. Spectra were taken in the standard "staring" mode, with four exposures at each of two positions, separated by one third of the slit length. A total of 8 individual spectra were taken in each sub-slit, for total on-source integration times of 480, 960, and 960 seconds.

Spectra were reduced using the S11 pipeline at the *Spitzer* Science Center, which includes ramp fitting, dark sky subtraction, droop correction, linearity correction, and wavelength calibration. One-dimensional spectra were extracted from the un-flatfielded two-dimensional spectra using the SMART data reduction package (Higdon et al. 2004). The extractions are then flux calibrated with the IRS spectrum of a star (α Lac), extracted in an identical manner using SMART. The data have been sky-subtracted by differencing the two nod positions along the slit, before spectral extraction. As a final step, we have scaled the SL-1 and LL-2 1D spectra by 3% and 8%, respectively, to match the LL-1 spectrum in the overlap region and produce a single low-resolution spectrum from $7.5 - 38\mu$m (observed frame).

Mid-IR photometry of FSC10214+4724 at 3.6, 4.5, 5.8 and 8.0 μm was obtained on 20 May 2004 using the Infrared Array Camera (IRAC; Fazio et al. 2004). The galaxy was observed in full array mode with a cyclic 5 point dither pattern resulting in a total on source integration time of 1 minute per filter. The source was unresolved and its Full-Width at Half Maximum (FWHM) varied between 1.5″and 2″. We performed photometry on the final mosaics produced by the SSC pipeline (S11.0.2) using an aperture of 3.6 arcseconds radius following the method described in the IRAC data Handbook. The resulting flux densities are accurate to <5%. No attempt was made to correct the IRAC photometry for the contribution of the lensing galaxy which is unresolved from the source.

3. Results

We plot the IRS spectrum of FSC 10214+4724 in Figure 1. The most prominent feature is a steep rise at the red end ($\sim 8 - 10~\mu$m rest wavelength). Extending the spectral energy distribution (SED) with the IRAS 60 and 100 μm photometry (Moshir & et al. 1990) makes clear that there is not simply a steeply rising continuum, but rather is a broad emission feature on top of a somewhat less steep continuum. We identify this feature as silicate emission, centered at $\sim 10~\mu$m. It is difficult to measure an accurate equivalent width for the feature, because the IRS wavelength coverage does not extend far enough to the red.

Three weak emission lines are also present. We identify the narrow emission line at rest wavelength 7.65 μm as the [Ne VI] fine structure line. This line has a rest-frame equivalent width (EW) of 0.02 μm, roughly comparable to that observed in low redshift Seyferts (Sturm et al. 1999; Lutz et al. 2000). The emission feature observed at $\sim 5.5~\mu$m in the rest-frame appears to be marginally resolved. We identify it as a blend of [Mg VII] and [Mg V] at 5.503 and 5.610 μm, respectively. These lines have been seen in nearby AGN (Sturm et al. 2002) and have ionization potentials of about 186 and 105 eV, similar to the 158 eV ionization potential of [Ne VI]. While there is also a rotational transition of H_2 at 5.51μm (the S(7) line) which is often quite strong in ULIRGs, this feature is always accompanied by much stronger emission from the other, lower transition, H_2 rotational lines, which are not present. The rest-frame equivalent width of the [Mg VII] and [Mg V] lines combined is $\sim 0.03 \pm 0.01~\mu$m. While uncertain, this EW appears to be a factor of 3-5 higher than in local AGN (Sturm et al. 2002). The EW of the Ne and Mg lines is a factor of a few higher than the strongest of the narrow, high-excitation emission lines (C IV, He II, [Ne IV]) seen in the rest-frame UV spectrum of FSC 10214+4724 (Rowan-Robinson et al. 1991; Goodrich et al. 1996).

There is a marginal detection of broad emission at 6.2 μm rest-frame, corresponding to the wavelength of polycyclic aromatic hydrocarbon (PAH) emission. Although the feature is clearly visible in Figure 1, examination of the individual extractions shows that it is more prominent in LL-2 than in LL-1. The observed wavelength (20.3 μm) places the feature near the noisy blue end of LL-1, but at a wavelength that is usually regarded as reliable. We take the measurement, $EW \sim 0.1~\mu$m in the rest-frame, as an upper limit. We also note that the corresponding 7.7 and 8.6 μm PAH emission features are not seen, despite being redshifted into a clean part of the spectrum and the fact that they are usually 1.5–2 times stronger than the 6.2 μm feature in starburst-dominated low redshift ULIRGs. The low ratio of 7.7 to 6.2 μm PAH equivalent width, while highly unusual, is not impossible under certain conditions (Kessler-Silacci et al. 2005). The 11.3 μm PAH feature might also be expected, but that line falls near the red end of LL-1 where the noise precludes a meaningful limit. Nonetheless, the lack of other PAH lines indicates that the 6.2 μm feature should be treated with caution.

4. Discussion

The shape of the SED of FSC 10214+4724 is dominated by dust at a variety of temperatures. Substantial cold dust must be present, given the strong emission at long wavelengths (> 40 μm, rest-frame; e.g., Rowan-Robinson et al. 1993). At the same time, warmer dust will be required to explain the 5-10 μm continuum. Dust warmer than 100 K can produce the silicate emission (e.g., Li & Draine 2001), but a hot dust component (several hundred K) is required to explain the ~ 5 μm continuum. The rest-frame near-infrared (NIR) will have a contribution from both star light and hot dust.

We have fit the SED with a multi-component model which includes three graphite and silicate dust grain components and a 3500K blackbody stellar component (Marshall et al. 2006). The three dust components in the model are not meant to represent three distinct physical structures, but rather they are indicative of the average temperature ranges within the source. The model was fit to the SED from observed frame NIR to millimeter wavelengths (see Figure 2. NIR data included the photometry of Soifer et al. (1991) and the IRAC data described in Section 2. Longer wavelength data included IRAS photometry at 60 and 100 μm, the 350 μm detection of Benford et al. (1999), and the sub-mm and mm data of Rowan-Robinson et al. (1993) and Downes et al. (1992).

A minimum of three dust components are required to fit the FSC 10214+4724 SED, one at ~ 50 K (cold), one at ~ 190 K (warm), and one at ~ 640 K (hot). Their relative contributions to the bolometric luminosity are given in Table 1 . Note that hot dust contribution is an upper limit, because it is dominated by the IRAC data and no correction has been made for contamination by the foreground lensing galaxy. The stellar emission is a negligible contribution to the bolometric luminosity, but is needed to fit the shortest wavelength data. component. The cold dust component (51 ± 6 K) is in good agreement with the estimate of Benford et al. (1999), 55 K. Each component contains a distribution of grains with different equilibrium temperatures depending on their size and composition. Additionally, each component contains emission from dust at different radial distances, and therefore temperatures, from the illuminating source. We define the characteristic temperature of a component to be the temperature of the most luminous grain size at the distance from the source contributing the majority of the luminosity. This luminosity dominating distance corresponds to a $\tau(UV) \sim 0.5$, where approximately half of the UV-source photons have been absorbed. Each component therefore contains dust above and below the characteristic temperature. With this definition, the characteristic temperature roughly corresponds to the expected peak in the dust modified (grey-body) Planck function.

The observed SED of FSC 10214+4724 appears consistent with low redshift, AGN-dominated ULIRGs. Such sources can have cold dust components which account for up to

40% of the bolometric luminosity, due to both AGN-heated cold dust far from the nucleus and the presence of a small underlying starburst (Armus et al. 2004, 2006). Rowan-Robinson (2000) also estimates that the AGN contributes most of the luminosity of FSC 10214+4724. In addition, FSC 10214+4724 shows silicate emission, similar to other AGN observed with the IRS, and a hot (graphite) dust continuum. However, the hot dust contribution is quite small compared to many AGN-dominated ULIRGs or QSOs. The only obvious fine-structure lines are [Ne VI], [Mg VII] and [Mg V], high-ionization species not observed in starburst galaxies. There is little if any PAH emission. The upper limit to the $6.2\mu m$ EW is approximately a factor of $5 - 10$ lower than most pure starburst galaxies (Brandl et al. 2005) and ULIRGs dominated by star formation (Armus et al. 2004, 2006).

However, differential magnification is likely to be enhancing the central AGN, reducing the PAH EW and making the silicate emission more obvious in the IRS spectrum. Eisenhardt et al. (1996) estimate a magnification factor of ~ 100 for the central 40 pc, but only a factor of ~ 30 out to at least 240 pc. The intrinsic contribution of the starburst to the bolometric luminosity could be larger than that inferred by our current model. We assume that the warm and hot dust heated by the AGN are magnified by an additional factor of 3.3, but that both the cold dust heated by the AGN and any dust heated by starburst are not. The ratio of cold to warm dust in local AGN- and starburst-dominated ULIRGs is approximately 2:3 and 3:1, respectively (Armus et al. 2006, in preparation). Taking these assumptions together, we estimate the intrinsic AGN contribution to the bolometric luminosity of FSC 10214+4724 to be $\sim 35\%$ after correction for the differential magnification. If the differential magnification factor is correct, this AGN contribution is probably an upper limit because AGN-dominated ULIRGs often have measurable starbursts.

If the starburst contributes 65% of the intrinsic luminosity, it is surprising that little or no PAH emission is seen. Taking our limit of 0.1 $\mu m > EW_{rest}$ and a differential magnification factor of 3.5 would place the limit of the EW for PAH emission within the range of other star-forming ULIRGs(Armus et al. 2005, in prep; Brandl et al. 2005). However, the uncertainty in our PAH measurement leaves this possibility unconfirmed; a lower signal to noise ratio would have made our limit higher. Furthermore, the lack of evidence for comparably strong PAH emission at 7.7 μm makes it likely that the EW at 6.2 μm is overestimated. Nonetheless, the limit demonstrates that substantial star formation can be present in FSC 10214+4724 and not visible in the (differentially magnified) IRS spectrum.

In figure 3, we compare the rest frame MIR spectrum of FSC 10214+4724 to the IRS spectra of three other sources. The intrinsic spectrum of FSC 10214+4724 is redder than the observed spectrum, given the differential magnification, so the differences seen in the figure would be greater if corrected for lensing. The comparison sources are an AGN-dominated

ULIRG (FSC 15307+3252), a silicate-emitting QSO (PG 1351+640) and a pure starburst galaxy (NGC 7714). PG 1351+640 has similar silicate emission, but has a much stronger hot dust continuum at ~ 5 μm (Hao et al. 2005). In fact, the cold dust emission in FSC 10214+4724 gives it a much steeper mid-to-far infrared slope than most AGN with silicate emission. The 30 μm to 6 μm flux density ratio of 46 in FSC 10214+4724, is higher than the reddest of the quasars in Hao et al. (2005) or Siebenmorgen et al. (2005), with a ratio of 11, and the reddest AGN in Weedman et al. (2005), NGC 1275, which has a ratio of 30. The ULIRG FSC 15307+325 has a similar MIR slope to FSC 10214+4724 in the 2-10 μm region, but has silicate absorption rather than emission, and a much weaker cold dust continuum at longer wavelengths. The continuum of NGC7714 is very red with a 30 μm to 6 μm flux density ratio of 120, and a strong stellar contribution at the short wavelengths.

In many AGN-dominated ULIRGs, the MIR spectrum is even bluer, with a strong continuum in the ~ 5 μm region (e.g., Laurent et al. 2000). ULIRGs with steeper mid-infrared continua tend also to have silicate absorption, not emission. We see no evidence in the spectrum of FSC 10214+4724 for an underlying silicate absorption feature at 9.7 μm. Furthermore, the profile of the silicate emission is consistent with that seen in most other AGN observed with the IRS (Hao et al. 2005; Siebenmorgen et al. 2005; Weedman et al. 2005); although see Sturm et al. (2005) for a counter example and discussion of the factors influencing the profile shape. While some absorption may be filled in with emission, the absorption and emission profiles are not necessarily identical. A coincidence of opacity, temperature, and grain mixture in the emitting and absorbing regions would be required.

The AGN contribution to the bolometric luminosity in FSC 10214+4724 is apparently substantial but does not dominate. Nonetheless, the PAH emission expected for a starburst is weak or absent. An unusual dust geometry would be required for an AGN alone to explain the SED, given the amount of cold dust. The other available evidence points to a standard AGN configuration. The shape of the spectrum between $2 - 12\mu$m is qualitatively similar to dusty torus models (Pier & Krolik 1992) with inner radius to height ratios of $a/h \sim 0.3$, and opening angles of $\sim 50°$– consistent with a high-luminosity equivalent of Seyfert 2 galaxy, like NGC 1068. The similarlity to NGC 1068 hass previously been noted(e.g., Barvainis et al. 1995). The presence of silicate emission in the IRS spectrum rules out models where the torus is seen edge-on, or where the AGN is completely obscured by foreground (cold) dust.

REFERENCES

Alexander, D. M., Chartas, G., Bauer, F. E., Brandt, W. N., Simpson, C., & Vignali, C. 2005, MNRAS, 357, L16

Armus, L., et al. 2004, ApJS, 154, 178

Armus, L., et al. 2006 in prep.

Barvainis, R., Antonucci, R., Hurt, T., Coleman, P., & Reuter, H.-P. 1995, ApJ, 451, L9

Benford, D. J., Cox, P., Omont, A., Phillips, T. G., & McMahon, R. G. 1999, ApJ, 518, L65

Brandl, B. R., et al. 2004, ApJS, 154, 188

Brandl, B.R., et al. 2005, ApJ, (submitted)

Broadhurst, T., & Lehar, J. 1995, ApJ, 450, L41

Downes, D., Radford, J. E., Greve, A., Thum, C., Solomon, P. M., & Wink, J. E. 1992, ApJ, 398, L25

Eisenhardt, P. R., Armus, L., Hogg, D. W., Soifer, B. T., Neugebauer, G., & Werner, M. W. 1996, ApJ, 461, 72

Elston, R., McCarthy, P. J., Eisenhardt, P., Dickinson, M., Spinrad, H., Januzzi, B. T., & Maloney, P. 1994, AJ, 107, 910

Fazio, G. G., et al. 2004, ApJS, 154, 10

Goodrich, R. W., Miller, J. S., Martel, A., Cohen, M. H., Tran, H. D., Ogle, P. M., & Vermeulen, R. C. 1996, ApJ, 456, L9

Graham, J. R., & Liu, M. C. 1995, ApJ, 449, L29

Green, S. M., & Rowan-Robinson, M. 1996, MNRAS, 279, 884

Hao, L., et al. 2005, ApJ, 625, L75

Higdon, S. J. U., et al. 2004, PASP, 116, 975

Houck, J. R., et al. 2004, ApJS, 154, 18

Iwamuro, F., Maihara, T., Tsukamoto, H., Oya, S., Hall, D. N. B., & Cowie, L. L. 1995, PASJ, 47, 265

Kessler-Silacci, J. E., et al. 2005, ApJ in press; astro-ph/0511092

Kroker, H., Genzel, R., Krabbe, A., Tacconi-Garman, L. E., Tecza, M., Thatte, N., & Beckwith, S. V. W. 1996, ApJ, 463, L55

Lacy, M., Rawlings, S., & Serjeant, S. 1998, MNRAS, 299, 1220

Laurent, O., Mirabel, I. F., Charmandaris, V., Gallais, P., Madden, S. C., Sauvage, M., Vigroux, L., & Cesarsky, C. 2000, A&A, 359, 887

Lawrence, A., et al. 1993, MNRAS, 260, 28

Li, A., & Draine, B. T. 2001, ApJ, 554, 778

Lutz, D., Sturm, E., Genzel, R., Moorwood, A. F. M., Alexander, T., Netzer, H., & Sternberg, A. 2000, ApJ, 536, 697

Marshall, J.A., et al. 2005 in prep.

Moshir, M., et al. 1990, IRAS Faint Source Catalogue, version 2.0 (1990), 0

Nenkova, M., Ivezić, Ž., & Elitzur, M. 2002, ApJ, 570, L9

Pier, E. A., & Krolik, J. H. 1992, ApJ, 401, 99

Rowan-Robinson, M., et al. 1991, Nature, 351, 719

Rowan-Robinson, M., et al. 1993, MNRAS, 261, 513

Rowan-Robinson, M. 2000, MNRAS, 316, 885

Scoville, N. Z., Yun, M. S., Brown, R. L., & vanden Bout, P. A. 1995, ApJ, 449, L109

Serjeant, S., Lacy, M., Rawlings, S., King, L. J., & Clements, D. L. 1995, MNRAS, 276, L31

Siebenmorgen, R., Haas, M., Krügel, E., & Schulz, B. 2005, A&A, 436, L5

Soifer, B. T., et al. 1991, ApJ, 381, L55

Soifer, B. T., Cohen, J. G., Armus, L., Matthews, K., Neugebauer, G., & Oke, J. B. 1995, ApJ, 443, L65

Solomon, P. M., Downes, D., & Radford, S. J. E. 1992, ApJ, 398, L29

Sturm, E., Alexander, T., Lutz, D., Sternberg, A., Netzer, H., & Genzel, R. 1999, ApJ, 512, 197

Sturm, E., Lutz, D., Verma, A., Netzer, H., Sternberg, A., Moorwood, A. F. M., Oliva, E., & Genzel, R. 2002, A&A, 393, 821

Sturm, E., et al. 2005, ApJ, 629, L21

Vanden Bout, P. A., Solomon, P. M., & Maddalena, R. J. 2004, ApJ, 614, L97

Weedman, D., et al. 2005, ApJ, (submitted)

Table 1.   SED fit parameters

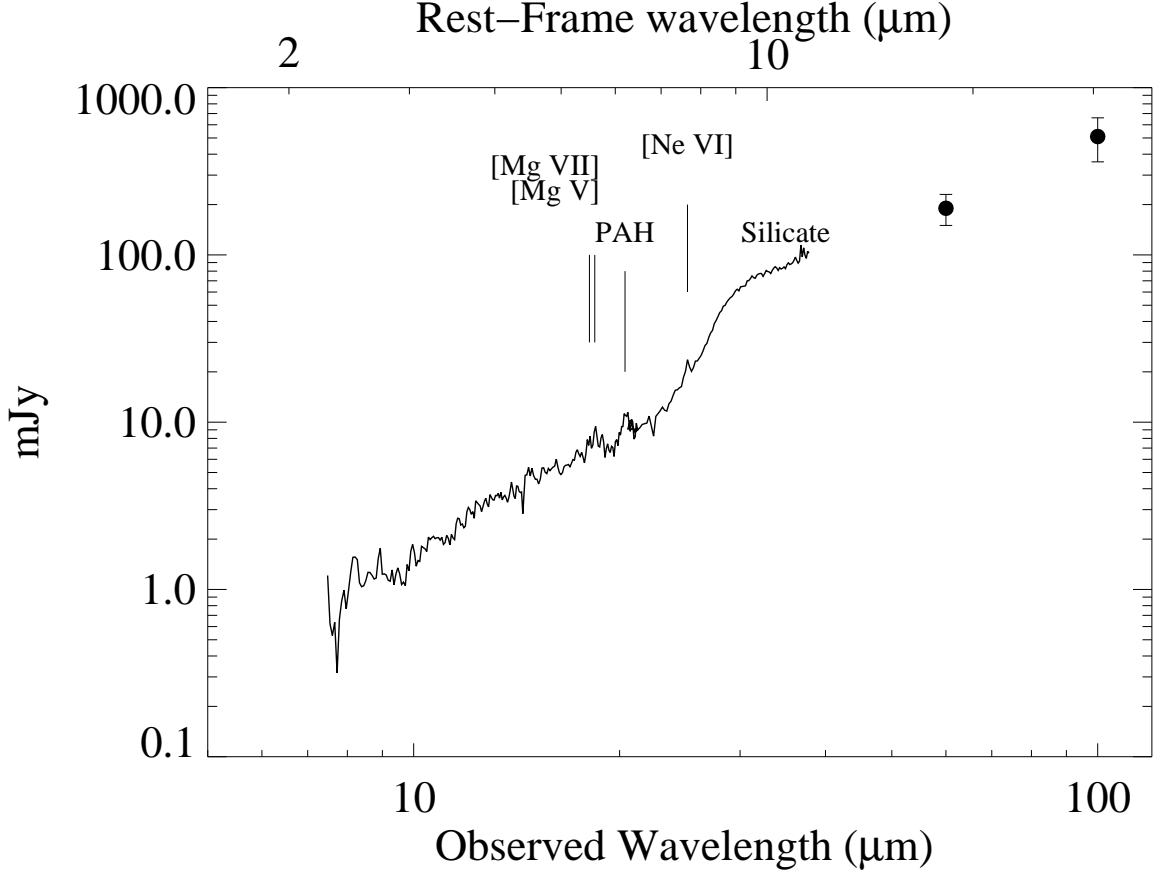| Dust Component	Temperature (K)	L/L_{tot} (%)
Hot	638 ± 20	5.6
Warm	191 ± 2	51.3
Cold	51 ± 6	43.3

Fig. 1.— The IRS spectrum and IRAS photometry of FSC 10214+4724. The extraction from the three modules, SL-1, LL-2 and LL-1, have been "stitched" together, cropping the noisier overlap wavelength regions. The filled circles show the IRAS photometry. Identified emission features are labeled.
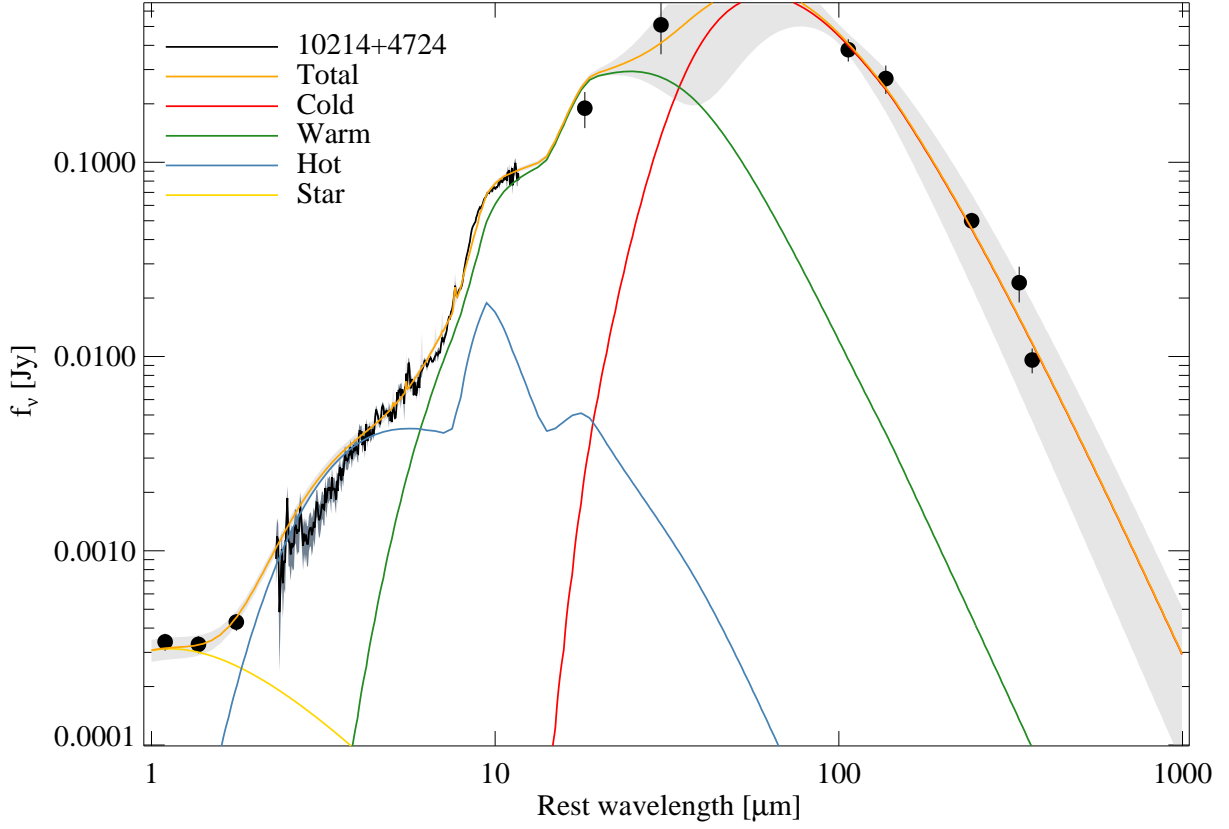
Fig. 2.— The semi-empirical dust model fit to the SED of FSC 10214+4724. The IRS mid-IR spectrum was extended with other data as described in the text. The components of the model (cold, warm, and hot dust, and stellar 3500K black body) are indicated in color. The shaded grey region indicates the 1σ uncertainty in the fit.
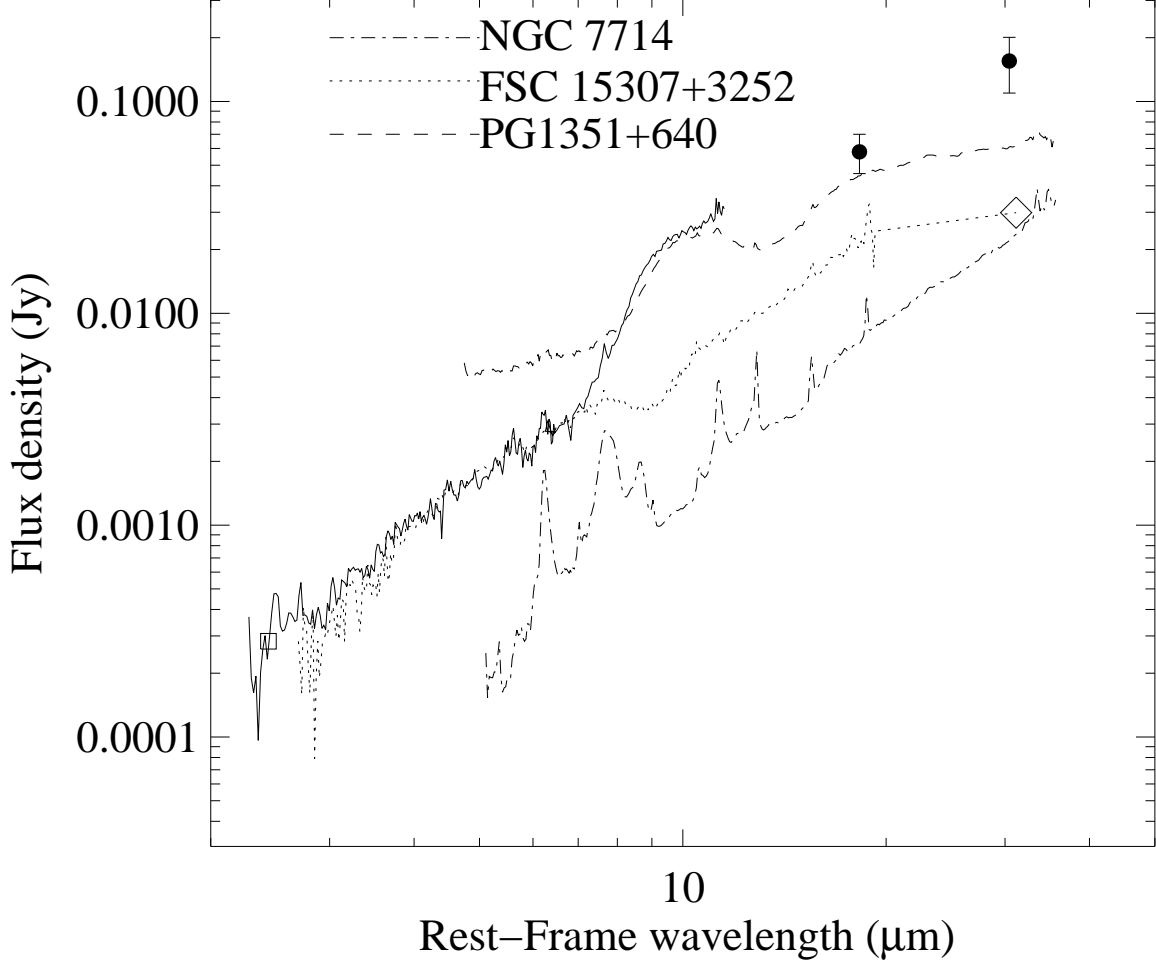
Fig. 3.— The SED of FSC 10214+4724 compared to other dusty galaxies observed with the IRS. We show the MIR spectrum of FSC 10214+4724 (solid line) and IRAS photometry (solid circles with error bars). For comparison, we overplot: the IRS spectrum of PG 1351+640 (dashed line; Hao et al. 2005), normalized to the prominent silicate emission; the IRS spectrum of the ULIRG FSC 15307+3252 (dotted line; Charmandaris 2005, in prep.) and its IRAS photometry (connected by dotted line, data point shown as open diamond) normalized at 5-7 μm; and the spectrum of NGC 7714 (dot-dashed line; Brandl et al. 2004), normalized at 5-7 μm and then offset by a factor of 5 for clarity. Note that the differential magnification causes the observed spectrum of FSC 10214+4724 to appear bluer than it would intrinsically, so the comparison in this figure should be taken as a lower limit.